AGN as potential factories for eccentric black hole mergers

https://doi.org/10.1038/s41586-021-04333-1

Received: 8 October 2020

Accepted: 10 December 2021

Published online: 9 March 2022



Check for updates

J. Samsing^{1⊠}, I. Bartos², D. J. D'Orazio¹, Z. Haiman³, B. Kocsis^{4,5}, N. W. C. Leigh^{6,7}, B. Liu¹, M. E. Pessah¹ & H. Taqawa⁸

There is some weak evidence that the black hole merger named GW190521 had a non-zero eccentricity^{1,2}. In addition, the masses of the component black holes exceeded the limit predicted by stellar evolution³. The large masses can be explained by successive mergers^{4,5}, which may be efficient in gas disks surrounding active galactic nuclei, but it is difficult to maintain an eccentric orbit all the way to the merger, as basic physics would argue for circularization⁶. Here we show that active galactic nuclei disk environments can lead to an excess of eccentric mergers, if the interactions between single and binary black holes are frequent⁵ and occur with mutual inclinations of less than a few degrees. We further illustrate that this eccentric population has a different distribution of the inclination between the spin vectors of the black holes and their orbital angular momentum at merger⁷, referred to as the spin-orbit tilt, compared with the remaining circular mergers.

Black holes that eventually merge in active galactic nuclei (AGN) disks can be brought into the disk through gas capture from the surrounding nuclear star cluster8 or can be produced through in situ star formation⁹⁻¹¹. Once a black hole is in the disk, it will undergo radial migration⁹ and can, as a result, pair up with another black hole to form a binary 12,13. Recent studies show that interactions between such migrating binary black holes and other single black holes in the AGN disk, referred to as binary-single interactions, likely provide the main pathway for bringing binaries to merger^{5,14-17} (Fig. 1). Despite progress on characterizing such interactions¹⁴, the inclusion of gravitational-wave emission during the interactions, which has been shown to be essential in resolving mergers with non-zero eccentricity that form in stellar clusters 18,19, remains unexplored. Observationally, GW190521 is among the first gravitational-wave sources with indications of an AGN disk origin^{3,20}. It is sensible to inquire whether its apparent non-zero eccentricity¹, as well as its observed approximately 90° spin-orbit tilt⁷, could arise naturally as a distinct signature, characteristic of dynamically induced AGN disk mergers.

With this motivation, we explore how binary black holes merge through binary-single interactions in AGN disk environments when gravitational-wave emission is included in the dynamics by means of the 2.5-post-Newtonian (2.5-PN) term²¹ (see Methods). To approach this complex astrophysical situation in a systematic way, we focus here on quantifying the unique signatures that might be associated with the roughly 2D disk-like environment of the AGN disk compared with the usual 3D interactions found in stellar clusters¹⁹. For this, we perform controlled experiments of initially circular black hole binaries interacting with singles incoming on an orbital plane that is inclined relative to the binary orbital plane by an angle ψ , for which $\psi = 0$ corresponds to a coplanar interaction (Fig. 4). For a given scattering, we study the characteristics of the merging black holes, which we divide into the following two distinct categories; 3-body merger: two of the three interacting black holes merge while they are all bound and interacting 19 (Fig. 1); 2-body merger: the binary black hole survives the three-body interaction, but merges before undergoing its next interaction²².

Figure 2 shows the probability for merger as a function of black hole binary semimajor axis, a. As shown in this figure, restricting the interactions to be coplanar leads to a notable enhancement of mergers; for example, for a binary with a semimajor axis $a \approx 1$ AU, the fraction of 3-body mergers is about 100 times larger in the 2D disk case compared with the 3D cluster case. As outlined in the Methods, this enhancement is due to the difference in eccentricity distributions of the dynamically assembled binaries. P(e), that follows $\approx e/\sqrt{1-e^2}$ in the 2D case, compared with $\approx 2e$ in the 3D case²³⁻²⁵. Our analytic approximations (see Methods) for both the 2-body and the 3-body merger probabilities, p_2 and p_3 , respectively, are also included in Fig. 2. Assuming the equal-mass limit, the corresponding ratio of probabilities between the 2D and the 3D cases is

$$\frac{p_2^{(2D)}}{p_2^{(3D)}} \approx 10^1 \times \left[\frac{m}{20 \, M_\odot} \right]^{-6/14} \left[\frac{a}{1 \, \text{AU}} \right]^{8/14} \left[\frac{t_{\text{int}}}{10^5 \, \text{years}} \right]^{-1/7}, \tag{1}$$

$$\frac{p_3^{(2D)}}{p_3^{(3D)}} \approx 10^2 \times \left[\frac{m}{20 \, M_\odot} \right]^{-5/14} \left[\frac{a}{1 \, \text{AU}} \right]^{5/14}, \tag{2}$$

in which m is the black hole mass and t_{int} is the time between interactions scaled to a value characteristic for AGN disk models⁵. These results show that the effects from breaking the scattering isotropy become increasingly important at larger a and smaller m. Note further the weak dependence on t_{int} .

An interesting observational consequence of the enhancement of the merger probabilities is the increase in the number of black hole mergers

Niels Bohr International Academy, Niels Bohr Institute, Copenhagen, Denmark. 2Department of Physics, University of Florida, Gainesville, FL, USA. 3Department of Astronomy, Columbia University, New York, NY, USA, 4Rudolf Peierls Centre for Theoretical Physics, Clarendon Laboratory, Oxford, UK, 5St Hugh's College, Oxford, UK, 6Departamento de Astronomía, Facultad Ciencias Físicas y Matemáticas, Universidad de Concepción, Concepción, Chile. ⁷Department of Astrophysics, American Museum of Natural History, New York, NY, USA. ⁸Astronomical Institute, Tohoku University, Sendai, Miyagi, Japan. [™]e-mail: jsamsing@gmail.com

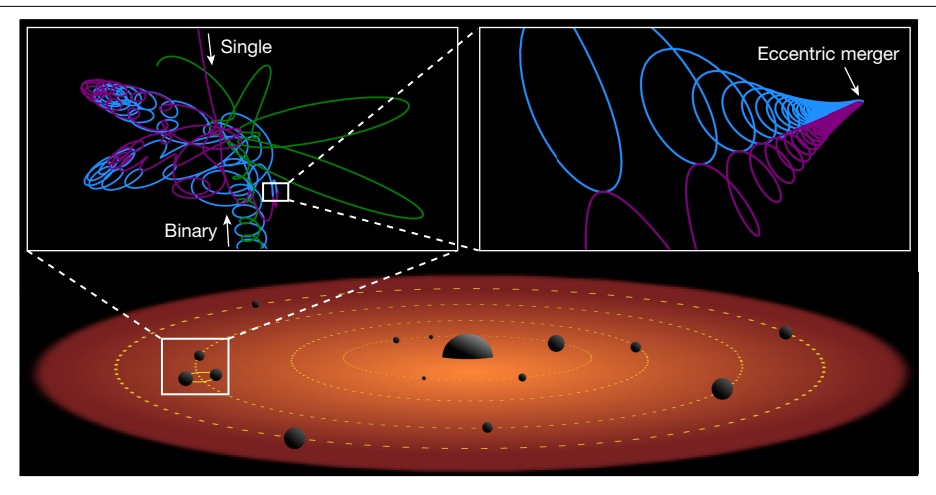


Fig. 1 | **Illustration of an eccentric LIGO-Virgo source forming in an AGN disk.** Bottom, AGN disk (not to scale) with its central supermassive black hole and a population of smaller orbiting black holes. These smaller black holes occasionally pair up to form binary black holes, which often undergo

scatterings with the single-black-hole population. Top, outcome of a [50 M_{\odot} , $80 M_{\odot}$] binary black hole interacting with an incoming [70 M_{\odot}] black hole, which results in a [80 M_{\odot} , 70 M_{\odot}] binary black hole merger during the interaction, with an eccentricity of about 0.5 in LIGO-Virgo.

with a measurable eccentricity, e, at gravitational-wave frequency f_{GW} . This is illustrated in Fig. 2, which includes the probability that a given scattering results in a merger with a measurable e in LIGO-Virgo (e > 0.1 at $f_{\text{GW}} \ge 10$ Hz). As shown in the figure, the eccentric population follows closely the 3-body merger population, but the scaling with m and a is slightly different. As a consequence, the probability of forming a merger with e > 0.1 at $f_{\text{GW}} \ge 10$ Hz in the 2D case is enhanced relative to the 3D case by the factor (see Methods)

$$\frac{p_{0.1.10\,\text{Hz}}^{(2D)}}{p_{0.1.10\,\text{Hz}}^{(3D)}} \approx 10^2 \times \left[\frac{m}{20\,M_\odot}\right]^{-1/6} \left[\frac{a}{1\,\text{AU}}\right]^{1/2}.\tag{3}$$

Figure 3 extends this analysis to the less-idealized case by plotting the merger probabilities as a function of ψ for fixed a = 1 AU. As shown

in the figure, ψ here must be \lesssim 1° for the boost in eccentric LIGO-Virgo mergers to be notable. The true distribution of ψ is observationally unconstrained, and it is unclear whether binary–single scatterings are within a few degrees of coplanar, as is necessary in our model. If the characteristic inclination angle is comparable with the AGN disk thickness h divided by the radius $r_{\rm H} \approx R(m/M)^{1/3}$ of the Hill sphere, in which R is the distance to the central supermassive black hole with mass M, then $\psi \approx 1^{\circ}$ for thin disk models^{5,26} ($h/R \approx 10^{-3}$, $M \approx 10^{6} M_{\odot}$, $m \approx 50 M_{\odot}$). If, instead, the characteristic inclination angle is given by h divided by the semimajor axis of the binary (as might happen if turbulent eddies and/or 2-body scattering are important), then $\psi \approx 1$ radian or more and interactions coplanar enough for our mechanism to operate are rare. It is uncertain whether gas drag will typically lead to efficient coplanar alignment, but if it does, then ψ less than a few degrees would be less rare.

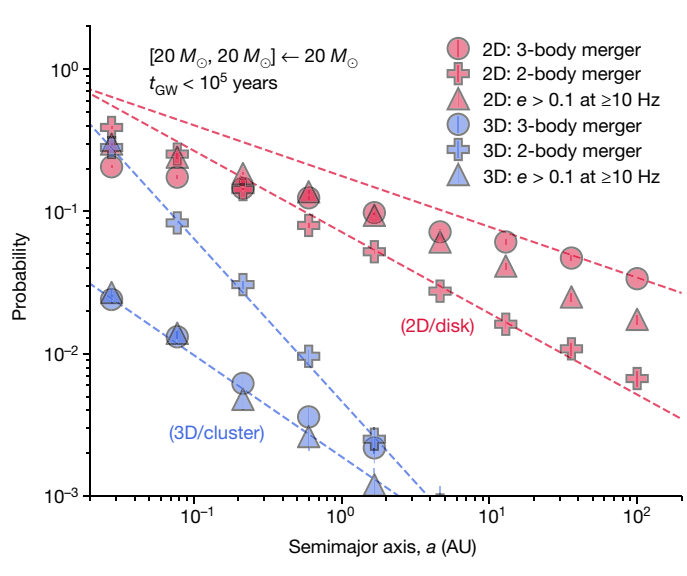


Fig. 2 | **Merger probability.** Probability of undergoing a 2-body merger (plus signs) or a 3-body merger (circles) with inspiral time $t_{\rm GW} < t_{\rm int} = 10^5$ years, derived from 2.5-PN binary–single interactions between black holes with equal mass $20\,M_{\odot}$, as a function of initial semimajor axis, a. The triangles show the probability of undergoing a merger with e > 0.1 at ≥ 10 Hz. Red, numerical results from 2D co-planar interactions; blue, numerical results from 3D isotropic interactions; dashed lines, analytical approximations (see Methods).

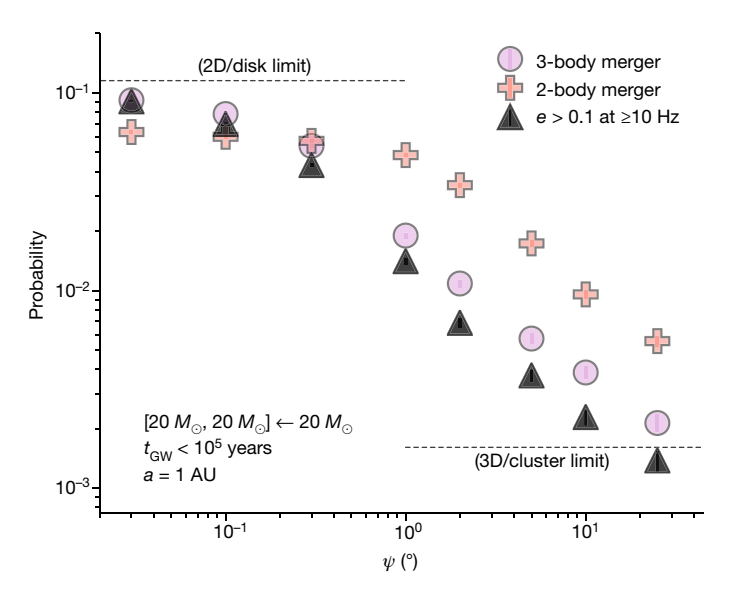


Fig. 3 | **Dependence on orbital inclination.** Probability of undergoing a 2-body merger (plus signs) or a 3-body merger (circles) with inspiral time $t_{\text{GW}} < t_{\text{int}} = 10^5$ years, derived from 2.5-PN interactions between a binary with a = 1 AU and an incoming single, for varying relative orbital inclination angle, ψ . The triangles show the probability of undergoing a merger with e > 0.1 at ≥ 10 Hz. All three objects are black holes with equal mass $m = 20~M_{\odot}$. The dotted lines illustrate the 2D (disk) and 3D (cluster) limits for the eccentric population (e > 0.1 at ≥ 10 Hz).

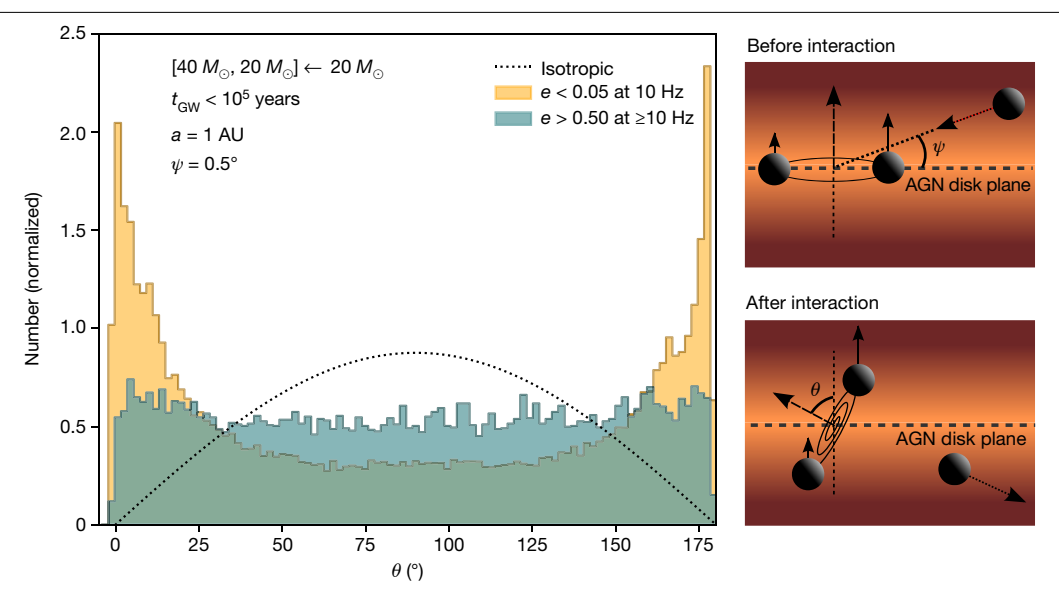


Fig. 4 | Distribution of orbital plane orientations. Results from 2.5-PN scatterings between an incoming $20 M_{\odot}$ black hole and a $[40 M_{\odot}, 20 M_{\odot}]$ binary black hole with a = 1 AU. The initial orbital inclination (depicted in top right panel) is set to $\psi = 0.5^{\circ}$. The histograms, each normalized, show the inclination angle between the orbital angular momentum vector of the final merging

binary black hole and the initial one, θ (depicted in lower right panel), where yellow and blue refer to the populations of merging binaries with eccentricity e < 0.05 at 10 Hz and e > 0.5 at ≥ 10 Hz, respectively. The dotted line shows for comparison an isotropic distribution expected in the 3D cluster-like case.

Finally, our 2.5-PN scatterings also show an interesting new relation between black hole merger eccentricity and spin-orbit tilt caused by the anisotropic environment provided by the AGN disk. The spin-orbit tilt is a powerful statistical measure of the underlying formation channel; for example, sources dynamically assembled in stellar clusters are expected to have an isotropic distribution, in contrast to mergers originating from isolated stellar binary evolution²⁷. Figure 4 explores this for AGN-disk-mediated mergers, by plotting distributions of the angle between the orbital angular momentum vector of the final merging binary black hole and that of the initial black hole binary, denoted θ , with Fig. 5 (see also Methods) showing the corresponding distributions of gravitational-wave frequency and eccentricity. We split the distributions in Fig. 4 into two categories based on binary eccentricity at the time of detectability, e < 0.05 at 10 Hz (yellow) and e > 0.5 at ≥ 10 Hz (blue). As seen in the figure, the distribution of θ with notable eccentricity in LIGO-Virgo (e > 0.5 population) is much broader and flatter than for the remaining circular (e < 0.05 population). Part of the reason for this is that eccentric mergers have a relatively small angular momentum vector, which can therefore be easily reoriented without being notably constrained by the (near coplanar) initial conditions, in contrast to the less eccentric mergers. The angle θ is not directly observable; however, the gas that brings the interacting black holes close to the plane of the

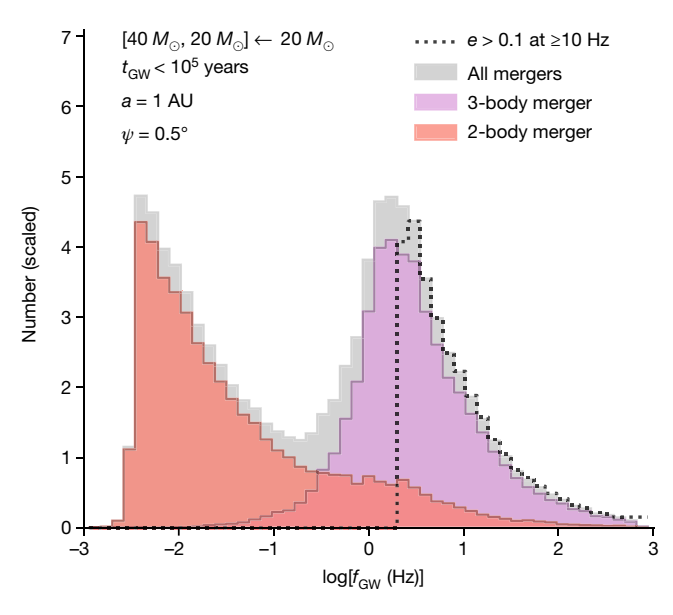
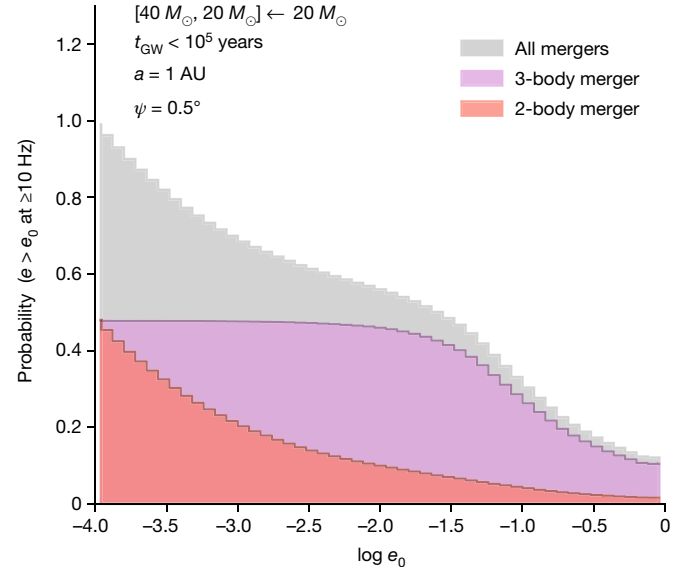


Fig. 5 | Eccentricity and gravitational-wave frequency distributions. Results from 2.5-PN scatterings, between an incoming $20 M_{\odot}$ black hole and a $[40 \, M_{\odot}, 20 \, M_{\odot}]$ binary black hole with initial $a = 1 \, \text{AU}$. The initial inclination between the binary and single orbital planes is $\psi = 0.5^{\circ}$. The red and purple distributions show the outcome from 2-body mergers and 3-body mergers with



 $t_{\rm GW} < t_{\rm int} = 10^5$ years, respectively, where grey is their sum. Left, distribution of binary black hole gravitational wave peak frequency, $f_{\rm GW}$, measured right after the time of assembly. Right, cumulative distribution of binary black hole orbital eccentricities at \geq 10 Hz. For sources formed with $f_{\rm GW}$ > 10 Hz, the corresponding eccentricity has been set to e=1.

Article

AGN disk before interaction swill also spin them up through accretion, which will drive their spin vectors towards being perpendicular to the AGN disk. As a result, θ is roughly equal to the observable spin-orbit tilt. This opens up the previously undescribed possibility of using eccentricity together with spin-orbit tilt to investigate the origin of AGN-disk-mediated mergers, and provides further a possible explanation for the non-zero eccentricity and noticeable spin-orbit tilt of GW190521 if it formed in an AGN disk.

Online content

Any methods, additional references, Nature Research reporting summaries, source data, extended data, supplementary information, acknowledgements, peer review information; details of author contributions and competing interests; and statements of data and code availability are available at https://doi.org/10.1038/s41586-021-04333-1.

- Gayathri, V. et al. Eccentricity estimate for black hole mergers with numerical relativity simulations. Nat. Astron. https://doi.org/10.1038/s41550-021-01568-w (2022).
- Romero-Shaw, I., Lasky, P. D., Thrane, E. & Calderón Bustillo, J. GW190521: orbital eccentricity and signatures of dynamical formation in a binary black hole merger signal. Astrophys. J. Lett. 903, L5 (2020).
- Abbott, R. et al. Properties and astrophysical implications of the 150M_o binary black hole merger GW190521. Astrophys. J. Lett. 900, L13 (2020).
- Yang, Y. et al. Hierarchical black hole mergers in active galactic nuclei. Phys. Rev. Lett. 123, 181101 (2019).
- Tagawa, H., Haiman, Z. & Kocsis, B. Formation and evolution of compact-object binaries in AGN disks. Astrophys. J. 898, 25 (2020).
- Peters, P. Gravitational radiation and the motion of two point masses. Phys. Rev. 136, B1224–B1232 (1964).
- Abbott, R. et al. GW190521: a binary black hole merger with a total mass of 150 M_o. Phys. Rev. Lett. 125, 101102 (2020).
- Bartos, I., Kocsis, B., Haiman, Z. & Márka, S. Rapid and bright stellar-mass binary black hole mergers in active galactic nuclei. Astrophys. J. 835, 165 (2017).
- Levin, Y. Formation of massive stars and black holes in self-gravitating AGN discs, and gravitational waves in LISA band. Preprint at https://arxiv.org/abs/astro-ph/0307084 (2003).

- Stone, N. C., Metzger, B. D. & Haiman, Z. Assisted inspirals of stellar mass black holes embedded in AGN discs: solving the 'final au problem'. Mon. Not. R. Astron. Soc. 464, 946–954 (2017).
- Cantiello, M., Jermyn, A. S. & Lin, D. N. C. Stellar evolution in AGN disks. Astrophys. J. 910, 94 (2021).
- McKernan, B., Ford, K. E. S., Lyra, W. & Perets, H. B. Intermediate mass black holes in AGN discs-I. Production and growth. Mon. Not. R. Astron. Soc. 425, 460-469 (2012).
- McKernan, B. et al. Constraining stellar-mass black hole mergers in AGN disks detectable with LIGO. Astrophys. J. 866, 66 (2018).
- Leigh, N. W. C. et al. On the rate of black hole binary mergers in galactic nuclei due to dynamical hardening. Mon. Not. R. Astron. Soc. 474, 5672–5683 (2018).
- Secunda, A. et al. Orbital migration of interacting stellar mass black holes in disks around supermassive black holes. Astrophys. J. 878, 85 (2019).
- Tagawa, H., Haiman, Z., Bartos, I. & Kocsis, B. Spin evolution of stellar-mass black hole binaries in active galactic nuclei. Astrophys. J. 899, 26 (2020).
- Kocsis, B., Gáspár, M. E. & Márka, S. Detection rate estimates of gravity waves emitted during parabolic encounters of stellar black holes in globular clusters. Astrophys. J. 648, 411–429 (2006).
- Rodriguez, C. L. et al. Post-Newtonian dynamics in dense star clusters: formation, masses, and merger rates of highly-eccentric black hole binaries. Phys. Rev. D 98, 123005 (2018).
- Samsing, J. Eccentric black hole mergers forming in globular clusters. Phys. Rev. D 97, 103014 (2018).
- Graham, M. J. et al. Candidate electromagnetic counterpart to the binary black hole merger gravitational-wave event S190521g. Phys. Rev. Lett. 124, 251102 (2020).
- Blanchet, L. Gravitational radiation from post-Newtonian sources and inspiralling compact binaries. Living Rev. Relativ. 17, 2 (2014).
- Samsing, J. & D'Orazio, D. J. Black hole mergers from globular clusters observable by LISA I: eccentric sources originating from relativistic N-body dynamics. Mon. Not. R. Astron. Soc. 481, 5445–5450 (2018).
- Monaghan, J. J. A statistical theory of the disruption of three-body systems II. High angular momentum. Mon. Not. R. Astron. Soc. 177, 583–594 (1976).
- 24. Valtonen, M. & Karttunen, H. The Three-Body Problem (Cambridge Univ. Press, 2006).
- Stone, N. C. & Leigh, N. W. C. A statistical solution to the chaotic, non-hierarchical three-body problem. *Nature* 576, 406–410 (2019).
- Thompson, T. A., Quataert, E. & Murray, N. Radiation pressure-supported starburst disks and active galactic nucleus fueling. Astrophys. J. 630, 167–185 (2005).
- Rodriguez, C. L., Zevin, M., Pankow, C., Kalogera, V. & Rasio, F. A. Illuminating black hole binary formation channels with spins in advanced LIGO. Astrophys. J. 832, L2 (2016).

Publisher's note Springer Nature remains neutral with regard to jurisdictional claims in published maps and institutional affiliations.

© The Author(s), under exclusive licence to Springer Nature Limited 2022

Methods

Analytical estimations and theoretical modelling

The coplanar 2D binary–single scattering setup, for which ψ = 0, not only represents the limiting case of our AGN disk scattering model but also leads also to an upper limit on the number of mergers compared with the isotropic 3D cluster case. Although idealized, it is therefore useful to consider this model to explore the expected maximum enhancement of the merger probability, when going from the cluster-like 3D case to the disk-like 2D case. In the following analytical treatment, we assume equal-mass binary components and omit the possible effects from gas drag in the dynamics^{28,29}.

We start by calculating the probability $P(t_{\rm GW} < \tau)$ that a dynamically assembled binary black hole has a gravitational-wave inspiral time $t_{\rm GW}$ less than some timescale τ . For an eccentric binary black hole, $t_{\rm GW}$ is given roughly by⁶

$$t_{\rm GW} \approx \frac{5c^5}{512G^3} \frac{a^4}{m^3} (1 - e^2)^{7/2} \approx t_{\rm c} \times (1 - e^2)^{7/2},$$
 (4)

in which e, a and m are the initial orbital eccentricity, semimajor axis and individual black hole mass, respectively, and $t_{\rm c}$ denotes the circular inspiral time for which e=0. The eccentricities of binary black holes dynamically assembled through 2D coplanar interactions are distributed as $^{23-25}$

$$P^{(2D)}(e) \approx e/\sqrt{1-e^2}$$
 (5)

from which it directly follows that

$$P^{(2D)}(t_{GW} < \tau) \approx (\tau/t_c)^{1/7},$$
 (6)

in which we have used that $P^{(2D)}(e > e_0) = \sqrt{(1-e_0^2)}$. With this expression, we can now estimate the probability that a binary black hole with given orbital parameters will merge through a 2-body or a 3-body merger process.

The probability of a 2-body merger, $p_2^{(2D)}$, is found by equating τ in equation (6) with the time until the binary black hole undergoes its next interaction, t_{int} ,

$$p_2^{(2D)} \approx (t_{\text{int}}/t_c)^{1/7} \approx 0.07 \left[\frac{t_{\text{int}}}{10^5 \text{ years}} \right]^{1/7} \left[\frac{m}{20 M_{\odot}} \right]^{3/7} \left[\frac{a}{1 \text{ AU}} \right]^{-4/7},$$
 (7)

in which we have normalized to values characteristic of AGN disk environments 5 . To estimate the 3-body merger probability, $p_3^{(2\mathrm{D})}$, we describe the often highly chaotic binary–single interaction as a series of $\mathcal N$ temporary states, each characterized by a binary black hole with a bound single 30 . Now, for one of these temporary binary black holes to merge, its inspiral time $t_{\rm GW}$ must be smaller than the characteristic timescale for the system 31,32 , T_0 ~ $\sqrt{a^3/(Gm)}$. Hence, the probability that a binary black hole undergoes a 3-body merger is found by first equating τ in equation (6) with T_0 and then multiplying by $\mathcal N$,

$$p_3^{(2D)} \approx \mathcal{N} \times (T_0/t_c)^{1/7} \approx 0.15 \left[\frac{m}{20 \, M_\odot} \right]^{5/14} \left[\frac{a}{1 \, \text{AU}} \right]^{-5/14}.$$
 (8)

For the last equality, we have used $\mathcal{N}\approx 20$ as found using the simulations introduced in Fig. 2 (we do not find \mathcal{N} to depend greatly on ψ for our considered equal-mass setups; however, it does depend on the mass hierarchy and should therefore be treated as a variable in the general case ³²). For comparison, in the isotropic 3D case, the eccentricity distribution P(e) instead follows ³³ $P^{(3D)}(e) = 2e$, from which one finds ¹⁹, $p_2^{(3D)}\approx (t_{\text{int}}/t_c)^{2/7}$ and $p_3^{(3D)}\approx \mathcal{N}\times (T_0/t_c)^{2/7}$. The relative change in going from 3D to the illustrative 2D case is therefore

$$\frac{p_2^{(2D)}}{p_2^{(3D)}} \approx (t_c/t_{\text{int}})^{1/7} \approx 10^1 \times \left[\frac{m}{20 \, M_\odot}\right]^{-6/14} \left[\frac{a}{1 \, \text{AU}}\right]^{8/14} \left[\frac{t_{\text{int}}}{10^5 \, \text{years}}\right]^{-1/7}, \quad (9)$$

$$\frac{p_3^{(2D)}}{p_3^{(3D)}} \approx (t_c/T_0)^{1/7} \approx 10^2 \times \left[\frac{m}{20 \, M_\odot}\right]^{5/14} \left[\frac{a}{1 \, \text{AU}}\right]^{5/14},\tag{10}$$

which shows here why a disk-like environment can lead to a notable enhancement of both 2-body and 3-body mergers. Comparing the relative probabilities,

$$(p_3^{(2D)}/p_2^{(2D)})/(p_3^{(3D)}/p_2^{(3D)}) \approx (t_{\text{int}}/T_0)^{1/7} > 1,$$
 (11)

we further conclude that the relative number of 3-body mergers forming in the 2D case is always greater than in the 3D case. This is important in relation to eccentric mergers, as will be described further below. Lastly, Fig. 2 illustrates the merger probabilities as a function of a, derived using our 2.5-PN N-body code³¹, together with our analytic approximations. As shown in this figure, we find excellent agreement in the large a limit as expected, as this is where the probabilities are small enough to be written as an uncorrelated sum over $\mathcal N$ states, as we did in equation (8).

One immediate consequence of the relative enhancement of 3-body mergers is a non-negligible population of binary black hole mergers that appear with a detectable eccentricity, $e_{\rm fr}$ at some gravitational-wave frequency, $f_{\rm GW}$. As for the merger probabilities above, we start by calculating an upper limit on the number of such eccentric mergers by again considering the illustrative 2D limit. For these calculations, we consider only the contribution from 3-body mergers, as they greatly dominate (Fig. 5).

For a binary black hole to appear with an eccentricity $e > e_{\rm f}$ at gravitational-wave peak frequency $f_{\rm GW} \approx \pi^{-1} \sqrt{2Gm/r_{\rm f}^3}$, in which $r_{\rm f}$ is the pericentre distance, the initial binary black hole pericentre distance at assembly (or 'capture') has to be smaller than $r_{\rm c}(e_{\rm f})$, for which $r_{\rm c}(e_{\rm f})$ at quadrupole order is given by 19,34

$$r_{\rm c}(e_{\rm f}) \approx \left(\frac{2Gm}{f_{\rm GW}^2 \pi^2}\right)^{1/3} \frac{1}{2} \frac{1 + e_{\rm f}}{e_{\rm f}^{12/19}} \left[\frac{425}{304} \left(1 + \frac{121}{304} e_{\rm f}^2\right)^{-1}\right]^{870/2299}$$
 (12)

Therefore the probability that a binary–single interaction results in an eccentric merger during the interaction is, to leading order, the probability that two of the three black holes form a temporary binary black hole with an initial pericentre $r_0 < r_c(e_f)$. To calculate this probability, denoted here in short by $p_{\rm ecc}$, we again describe the 3-body interaction as $\mathcal N$ temporary binary–single states and, by using that $P^{(2D)}(e>e_0) \approx \sqrt{2(1-e_0)}$ in the high-eccentricity 2D limit, together with the Keplerian relation $r_0/a=1-e_0$, we find 19

$$p_{\rm ecc}^{\rm (2D)} \approx \mathcal{N} \times \sqrt{\frac{2r_{\rm c}(e_{\rm f})}{a}}$$
 (13)

For $f_{\text{GW}} = 10 \text{ Hz}$, relevant for LIGO-Virgo³⁵,

$$p_{\rm ecc}^{\rm (2D)}(e > 0.1: \ge 10 \,\mathrm{Hz}) \approx 0.15 \left[\frac{m}{20 \,M_{\odot}} \right]^{1/6} \left[\frac{a}{1 \,\mathrm{AU}} \right]^{-1/2},$$
 (14)

in which this relation includes all sources that will appear with e > 0.1 at 10 Hz or above. Comparing this to the isotropic 3D case¹⁹ for which $p_{\rm ecc}^{(3D)} \approx \mathcal{N} \times 2r_{\rm c}(e_{\rm f})/a$, we find $p_{\rm ecc}^{(2D)}/p_{\rm ecc}^{(3D)} \approx \mathcal{N}/p_{\rm ecc}^{(2D)}$. Therefore, in the 2D case, the probability that a scattering results in an eccentric source is greater by at least a factor of about \mathcal{N} compared with the 3D case. These analytical considerations are further supported by the scattering

Article

results shown in Fig. 2. Finally, note that, for converting to the probability for actually observing an eccentric source, one has to sum the individual scattering probabilities — the ones we have considered so far — over the number of scatterings a given binary undergoes before merger takes place. The relative observable number of eccentric mergers is therefore greater than that stated above.

Results from unequal-mass scatterings

To illustrate that eccentric binary black hole mergers are not a unique outcome of the equal-mass interactions mainly presented in this article, we show here the results from 2.5-PN scatterings between a binary black hole $[40 \, M_{\odot}, 20 \, M_{\odot}]$ with $a = 1 \, \text{AU}$ and an incoming single $20 \, M_{\odot}$ black hole on an inclined orbital plane with $\psi = 0.5^{\circ}$. Figure 5 left shows the gravitational-wave peak frequency distribution at the time of dynamical formation (assembly) for each binary black hole that eventually merges. Nearly all 3-body mergers form near or in the LIGO-Virgo band, whereas the 2-body mergers peak at lower frequencies in the LISA band. Figure 5 right shows the corresponding cumulative eccentricity distribution at 10 Hz, in which we have assumed the quadrupole approximation⁶ for propagating the sources from their initial gravitational-wave peak frequency. As shown here, about 40% of all the binaries with merger time <10⁵ years will appear with an eccentricity e > 0.1 at $f_{GW} \ge 10$ Hz in this unequal-mass example. This is similar to what is found in the equal-mass case, which illustrates that the unequal-mass case is also expected to produce eccentric mergers at an enhanced rate when the interactions are near coplanar.

Post-Newtonian scattering simulations

We use a 2.5-PN *N*-body code that has been well tested and used in several previous studies³¹, including both 3-body³² and 4-body³⁶ dynamics. Although we had the option of including all lower-order PN terms up to 2.5, we included only the 2.5-PN term to both ensure stability¹⁸ and as this has been proved sufficient to accurately resolve and track the population of 3-body mergers that is unique to this channel³⁶. We did not include the possible effects from gas drag in the 3-body equations of motion, or tidal effects from the central supermassive black hole. 2D simulations of binaries in an AGN disk have been performed very recently³⁷, but an extension to the chaotic 3D few-body problem is highly non-trivial and will be the topic of future studies.

In all our 2.5-PN simulations, we limited the interaction time to 1,000 times the orbital time of the initial target binary, which resulted in only a few percent of inconclusive scatterings. These mainly originate from scatterings for which the third object is sent out on an almost unbound orbit with a corresponding orbital time that theoretically approaches infinity. These were therefore excluded from our sample. In addition, we only considered the strong-scattering regime, for which the single object on its first passage has an effective pericentre distance with respect to the binary that is similar to the binary semimajor axis. Therefore we do not include the regime of weak scatterings³⁸, which could take place during the early stages of the interaction when the single approaches the binary on a near corotating orbit, as could be the case from the AGN disk migration model. This naturally requires a more comprehensive N-body modelling of the problem, including effects from the disk and central black hole, and will be addressed in future studies.

For all our presented scatterings based on interactions between a binary and a single on a fixed orbital plane, we assume that the singles have an isotropic distribution of impact parameters at infinity. For the 3D isotropic scattering cases, the distribution is instead taken to be isotropic at a sphere at infinity. For all interactions, we randomized

the internal binary orbital phase angle; therefore, in this work, we do not distinguish between counterrotating and corotating interactions. We further assumed the single to nearly free-fall from infinity.

Data availability

The data that support the findings of this study are available from the corresponding author on reasonable request.

Code availability

Requests for codes should be addressed to the corresponding author.

- 28. Ostriker, E. C. Dynamical friction in a gaseous medium. Astrophys. J. 513, 252-258 (1999).
- Kim, H. & Kim, W.-T. Dynamical friction of a circular-orbit perturber in a gaseous medium. Astrophys. J. 665, 432–444 (2007).
- Samsing, J., MacLeod, M. & Ramirez-Ruiz, E. The formation of eccentric compact binary inspirals and the role of gravitational wave emission in binary-single stellar encounters. Astrophys. J. 784, 71 (2014).
- Samsing, J., MacLeod, M. & Ramirez-Ruiz, E. Formation of tidal captures and gravitational wave inspirals in binary-single interactions. Astrophys. J. 846, 36 (2017).
- Samsing, J., MacLeod, M. & Ramirez-Ruiz, E. Dissipative evolution of unequal-mass binary-single interactions and its relevance to gravitational-wave detections. Astrophys J. 853, 140 (2018).
- Heggie, D. C. Binary evolution in stellar dynamics. Mon. Not. R. Astron. Soc. 173, 729–787 (1975)
- Samsing, J., Askar, A. & Giersz, M. MOCCA-SURVEY database. I. Eccentric black hole mergers during binary-single interactions in globular clusters. Astrophys. J. 855, 124 (2018).
- Gondán, L. & Kocsis, B. Measurement accuracy of inspiraling eccentric neutron star and black hole binaries using gravitational waves. Astrophys. J. 871, 178 (2019).
- Zevin, M., Samsing, J., Rodriguez, C., Haster, C.-J. & Ramirez-Ruiz, E. Eccentric black hole mergers in dense star clusters: the role of binary-binary encounters. Astrophys. J. 871, 91 (2019)
- Li, Y.-P., Dempsey, A. M., Li, S., Li, H. & Li, J. Orbital evolution of binary black holes in active galactic nucleus disks: a disk channel for binary black hole mergers? Astrophys. J. 911, 124 (2021).
- Samsing, J., Hamers, A. S. & Tyles, J. G. Effect of distant encounters on black hole binaries in globular clusters: systematic increase of in-cluster mergers in the LISA band. *Phys. Rev.* D 100 (043010 (2019))

Acknowledgements We are grateful to N. Bose, K. Holley-Bockelmann, A. Pai, M. Zevin and M. Safarzadeh for their useful suggestions. J.S. is supported by the European Union's Horizon 2020 research and innovation programme under the Marie Skłodowska-Curie grant agreement no. 844629. D.J.D. received funding from the European Union's Horizon 2020 research and innovation programme under the Marie Skłodowska-Curie grant agreement no. 101029157 and through Villum Fonden grant no. 29466. I.B. acknowledges the support of the Alfred P. Sloan Foundation and NSF grants PHY-1911796 and PHY-2110060. H.T. is financially supported by the Grants-in-Aid for Basic Research by the Ministry of Education, Science and Culture of Japan (17H01102, 17H06360) and the Japan Society for the Promotion of Science (JSPS) KAKENHI grant number JP21J00794, N.W.C.L. acknowledges the support of a Fondecyt Iniciación grant 11180005, the financial support from Millenium Nucleus NCN19-058 (TITANs) and the BASAL Centro de Excelencia en Astrofisica y Tecnologias Afines (CATA) grant CATA AFB170002 along with ANID BASAL projects ACE210002 and FB210003, Z.H. acknowledges support from NASA grant NNX15AB19G and NSF grants AST-1715661 and AST-2006176, B.L. gratefully acknowledges support from the European Union's Horizon 2020 research and innovation program under the Marie Sklodowska-Curie grant agreement no. 847523 'INTERACTIONS'. This project has received funding from the European Research Council (ERC) under the European Union's Horizon 2020 research and innovation programme ERC-2014-STG under grant agreement no. 638435 (GalNUC) to B.K. M.E.P. gratefully acknowledges support from the Independent Research Fund Denmark (DFF) via grant no. DFF 8021-00400B.

Author contributions J.S. led the work, carried out the simulations and calculations, and wrote the initial manuscript together with I.B. and D.J.D. The remaining authors, Z.H., B.K., N.W.C.L., B.L., M.E.P. and H.T., all contributed equally to the intellectual development of the ideas and the preparation of the final manuscript.

Competing interests The authors declare no competing interests.

Additional information

Correspondence and requests for materials should be addressed to J. Samsing. **Peer review information** *Nature* thanks the anonymous reviewers for their contribution to the peer review of this work.

Reprints and permissions information is available at http://www.nature.com/reprints.